MODELING OF A LINEAR FORCE-FREE MAGNETIC FIELD IN A BOUNDED DOMAIN

V.I. Abramenko and V.B. Yurchishin
Crimean Astrophysical Observatory
334413, p/o Nauchny, Crimea, Ukraine

Abstract

A method for the reconstruction of the linear force-free magnetic field in a bounded domain (as a rectangular box Ω) is presented here. Dirichlet boundary value problem for the Helmholtz equation is solved for B_z component specified at the Ω boundary. Chebyshev's iteration method with the optimal rearrangement of the iteration parameters sequence was used. The solution is obtained as for the positive-definite, so for the non-sign-definite difference analogue of the differential operator $\nabla^2 u + \alpha^2 u$. Specifying two scalar functions B_x and B_y on the intersection of the lateral part of the Ω boundary with one selected plane $z = const$ and using B_z inside the Ω, we have found B_x and B_y throughout the Ω.

The algorithm was tested with the numerical procedure, which gives the analytic solution $\mathbf{B}$ of the linear force-free field (LFFF) equations for the dipole in a half-space. The root-mean-square deviation of the analytic solution $\mathbf{B}$ from the calculated $\mathbf{B}'$ does not exceed 1.0%. Boundary conditions for $\mathbf{B}'$ calculation were taken as given by the analytic LFFF solution $\mathbf{B}$. Comparison of $\mathbf{B}'$ with $\mathbf{B}''$, which was calculated by the potential non-photospheric boundary conditions, shown that they differ significantly. Thus, specification of boundary conditions at non-photospheric boundaries of the volume under consideration is of particular importance when modeling the LFFF in a bounded volume.

The algorithm proposed here allows to use the information about magnetic fields in the corona for the modeling of LFFF in a limited domain above an active region on the Sun.

1 Introduction

Along with a study of coronal magnetic fields on the basis of the indirect information provided by radio, white light and soft X-ray observations (see, e.g., the review by Alissandrakis, 1994), the modeling of coronal magnetic structures by photospheric field measurements remains a strong tool for the investigation of solar magnetic field. For the modeling one usually employs current-free or force-free approximation (see, e.g., reviews by Seehafer and Staude, 1983; Sakurai, 1989). Recently Aly and Seehafer (1993) proposed a new approach to calculate the magnetic field of the whole solar corona under the assumption that the field is force-free only inside closed domains above active regions being potential everywhere. In the modeling of linear force-free field (LFFF) above a limited region on the solar surface (i.e. above an active region) boundary conditions at lateral parts of the volume is a problem. The solution to LFFF equations is sensitive to the treatment of lateral boundary conditions (Seehafer, 1978; Seehafer, 1982). On the other hand, neither Fourier transform method, nor Green function method give a possibility to impose directly arbitrary lateral boundary conditions. A numerical routine, which allows to do it, should be handy in studying how changes in lateral boundary conditions influence on the LFFF solution, and in using of the information about coronal magnetic fields, which can be obtained from radio, white light and soft X-ray observations.

Here we present a numerical algorithm which renders it possible to calculate the LFFF in a bounded volume (as a rectangular box Ω) provided B_z are specified at all sides of the Ω and B_x, B_y are prescribed on the intersection of the lateral part of the Ω boundary with some plane $z = const$. The algorithm is based on the solution of the Dirichlet boundary value problem (DBVP) to the Helmholtz equation by the Chebyshev's iteration method.

2 Basic Formulation

The force-free field can be described by equations:

$$\begin{aligned} \nabla \times \mathbf{B} &= \alpha \mathbf{B} && (1)\\ \nabla \cdot \mathbf{B} &= 0. && (2) \end{aligned}$$

If the scalar quantity α is constant in space we have linear force-free field with the field vector satisfying the Helmholtz equation

$$\nabla^2 \mathbf{B} + \alpha \mathbf{B} = 0. \qquad (3)$$

Let us calculate a LFFF inside a rectangular box Ω: $\{x_0 \le x \le x_0 + L_x,\ y_0 \le y \le y_0 + L_y, z_0 \le z \le z_0 + L_z\}$. Let the bottom Σ_1 to bound the Ω by the plane $z = z_0$; the side Σ_2 to bound the Ω by the plane $y = y_0$; the side Σ_3 — by the plane $x = x_0 + L_x$; the side Σ_4 — by the plane $y = y_0 + L_y$; the side Σ_5 — by the plane $x = x_0$; the top Σ_6 — by the plane $z = z_0 + L_z$.

The uniform grid ω inside the Ω let be as

$$\begin{aligned} \omega \;=\; & \{x_i = x_0 + (i-1)h_1,\ i = 1, \ldots, n_1,\ L_x = (n_1 - 1)\, h_1; \\ & y_j = y_0 + (j-1)h_2,\ j = 1, \ldots, n_2,\ L_y = (n_2 - 1)\, h_2; \qquad (4)\\ & z_l = z_0 + (l-1)h_3,\ l = 1, \ldots, n_3,\ L_z = (n_3 - 1)\, h_3.\} \end{aligned}$$

We will calculate the LFFF inside the Ω under the assumption that B_z are specified at all sides of the Ω:

$$\begin{aligned} B_z|_{\Sigma_1} &= \psi_1(x, y) && (5)\\ B_z|_{\Sigma_2} &= \psi_2(x, z) && (6)\\ B_z|_{\Sigma_3} &= \psi_3(y, z) && (7)\\ B_z|_{\Sigma_4} &= \psi_4(x, z) && (8)\\ B_z|_{\Sigma_5} &= \psi_5(y, z) && (9)\\ B_z|_{\Sigma_6} &= \psi_6(x, y); && (10) \end{aligned}$$

and B_x, B_y are specified on the intersection G of the lateral part of the boundary of the Ω with one selected plane $z = z^*(z_0 \le z^* \le z_0 + L_z)$:

$$\begin{aligned} B_x|_G &= g_1(x, y)|_G && (11)\\ B_y|_G &= g_2(x, y)|_G && (12) \end{aligned}$$

The method proposed here imposes no constraints on the functions ψ in (5)-(10) and g in (11)-(12). Boundary conditions (5)-(12) may be chosen either vanishing, or potential, or force-free, or by some another way using *a priori* information about the field in the corona.

At first we calculated B_z throughout the Ω, and secondly, using B_z and (11)-(12), B_x and B_y components were computed.

2.1 Calculation of B_z

Every component of the LFFF satisfies the Helmholtz equation (3). So for B_z component we have to solve the DBVP for the Helmholtz equation:

$$\nabla^2 B_z + \alpha^2 B_z \quad = \quad 0, \tag{13}$$

where ∇^2 denotes the $3D$ Laplacian in Cartesian coordinates: $\nabla^2 = \frac{\partial^2}{\partial x^2} + \frac{\partial^2}{\partial y^2} + \frac{\partial^2}{\partial z^2}$. Boundary conditions are specified by (5)-(10).

Let us denote $u \equiv B_z$. The difference analogue of the differentiation operator $A\,u \equiv \nabla^2 u + \alpha^2 u$ on the grid ω can be defined as

$$\begin{aligned} \mathcal{A}\,u \quad = \quad & (u_{i+1,j,l} - 2u_{i,j,l} + u_{i-1,j,l})/h_1^2 + \\ & (u_{i,j+1,l} - 2u_{i,j,l} + u_{i,j-1,l})/h_2^2 + \\ & (u_{i,j,l+1} - 2u_{i,j,l} + u_{i,j,l-1})/h_3^2 + \alpha^2\, u_{i,j,l}, \\ & i = 2,3\ldots,n_1-1,\ j = 2,3\ldots,n_2-1, l = 2,3\ldots,n_3-1. \end{aligned} \tag{14}$$

The spectrum of the operator $\mathcal{A}\,u$ is well known (Samarsky and Nikolaev, 1978, p.470):

$$\mu_k = \lambda_k - \alpha^2, \tag{15}$$

since eigenvalues λ_k of the 3D Laplacian are given by

$$\lambda_k \quad = \quad \lambda_{k_1}^{(1)} + \lambda_{k_2}^{(2)} + \lambda_{k_3}^{(3)},\ k = 1,2,\ldots,n_1 \times n_2 \times n_3 \tag{16}$$

$$\lambda_{k_\gamma}^{(\gamma)} \quad = \quad \frac{4}{h_\gamma^2} \sin^2 \frac{k_\gamma \pi}{2n_\gamma},\ k_\gamma = 1,2,\ldots,n_\gamma;\ \gamma = 1,2,3. \tag{17}$$

Minimum and maximum eigenvalues of the $3D$ Laplacian are

$$\min_k \lambda_k \equiv \delta \quad = \quad \sum_{\gamma=1}^{3} \frac{4}{h_\gamma^2} \sin^2(\pi/2n_\gamma), \tag{18}$$

$$\max_k \lambda_k \equiv \Delta \quad = \quad \sum_{\gamma=1}^{3} \frac{4}{h_\gamma^2} \cos^2(\pi/2n_\gamma). \tag{19}$$

If $\alpha^2 < \delta$, then $\mu_k > 0$ for all $k = 1,2,\ldots,n_1 \times n_2 \times n_3$, i.e., the operator $\mathcal{A}\,u$ is positive-definite. A solution of this DBVP is well known to exist and to be unique. Stable algorithms to solve difference equations with such operators are developed. Later, in the Subsection 2.1.1, we apply one of them for our purpose.

If $\alpha^2 > \delta$, then, at first, a solution of the DBVP (13), (5)-(10) exists and is unique if and only if $\alpha^2 \neq \lambda_k, k = 1, 2, \ldots, n_1 \times n_2 \times n_3$. And the secondary, some eigenvalues μ_k are negatives, thus the operator $\mathcal{A}\,u$ is non-sign-definite. To solve the DBVP with such an operator the specific procedures are required. One of them is demonstrated in the Subsection 2.1.2.

For our case, when the bounds of the spectrum of the difference operator $\mathcal{A}\,u$ are known, and one know nothing about a start approach u_0 inside the domain of integration Ω, it is better to use the Chebyshev's two-level iteration method (Samarsky and Nikolaev, 1978).

2.1.1 The case of positive-definite difference operator, $\alpha^2 < \delta$.

To solve the equation $A\,u = 0$ with non-degenerate linear operator $A\,u$, which is represented on the grid ω by the positive-definite difference operator $\mathcal{A}\,u$, let us create the explicit iteration scheme (Samarsky and Nikolaev, 1978):

$$u_{m+1} = u_m + \tau_{m+1} \cdot \mathcal{A}\,u_m, \quad m = 0, 1, 2, \ldots, n \tag{20}$$

with an arbitrary starting function u_0; m is a running iteration number, n is a total number of iterations; $\mathcal{A}\,u$ is defined by (14); $\{\tau_{m+1}\}$ is a sequence of iteration parameters. The latters are given by

$$\tau_m = \frac{\tau_0}{(1 + \rho_0\,\nu_m)}, \tag{21}$$

where

$$\tau_0 = 2/(\gamma_1 + \gamma_2),\ \rho_0 = (1 - \xi)/(1 + \xi),\ \xi = (\gamma_1)/(\gamma_2), \tag{22}$$

γ_1 and γ_2 are the lower and upper bounds of the spectrum of the operator $\mathcal{A}\,u$. For our case they are

$$\gamma_1 = \delta - \alpha^2,\ \ \gamma_2 = \Delta - \alpha^2. \tag{23}$$

The total number of iterations n is determined by the *a priori* given value ε characterizing the accuracy of calculations:

$$n \geq n_0(\varepsilon) = \ln(2/\varepsilon)/\ln(1/\rho_1), \tag{24}$$

where

$$\rho_1 = (1 - \sqrt{\xi})/(1 + \sqrt{\xi}). \tag{25}$$

In (21) ν_m belong to the set $\mathcal{M}_n$ of roots of the Chebyshev's polynomial $T_n(x)$ of the first kind of degree n:

$$T_n(x) = \begin{cases} \cos(n\ \arccos(x)), & |x| \leq 1, \\ \cosh(n\,Arch(x)), & |x| \geq 1, \end{cases} \tag{26}$$

$$\nu_m \in \mathcal{M}_n,\ \mathcal{M}_n = \{-\cos\frac{2i-1}{2n}\pi,\ i = 1, 2, \ldots, n\}. \tag{27}$$

All elements of $\mathcal{M}_n$ have to be chosen as ν_m.

The stability of the iteration process (20) significantly depends on the order of the taking of ν_m out of $\mathcal{M}_n$. The matter is that the norm $||S||$ of an operator of the transition from an iteration to the next iteration can become greater than 1.0 for some m, what leads to the growth of computational errors. It is worth to arrange $\{\tau_m\}$ in such an order that every transition with $||S|| > 1$ is followed by the transition with $||S|| < 1$. Then computational errors are not accumulate and the iteration process is stable. A technique for optimal arrangement of $\{\tau_m\}$ is given in Appendix.

When the optimal sequence $\{\tau_m\}$ is formed and a start approach u_0 is specified (say, $u_0 = 0$ in all internal nodal points of the grid ω), one can begin the iteration process according to the scheme (20).

2.1.2 The case of non-sign-definite difference operator, $\alpha^2 > \delta$.

An approach to solve a grid equation $\mathcal{A}\,u = 0$ with a non-sign-definite difference operator may be as follows (Samarsky and Nikolaev, 1978). For the given non-sign-definite operator $\mathcal{A}$ we set up an operator

$$\hat{\mathcal{A}} = \mathcal{A}^2 - 2\,\beta\,\mathcal{A}, \tag{28}$$

where the parameter β has to be fitted so that $\hat{\mathcal{A}}$ being a positive-definite operator. The iteration scheme for an equation with such an operator is well known (see, for example, the above Subsection). By making use of this scheme and taking into account (28) one may form the iteration scheme to solve the equation with non-sign-definite operator. It comes only to the complication of the sequence of iteration parameters $\{\tau_m\}$. Below we present the formulae for calculating of $\{\tau_m\}$ for this case.

Let us suppose that $\alpha^2 \neq \lambda_k$, where λ_k are determined by (16), (17). Then the equation (13) has a unique solution in the Ω satisfying the boundary conditions (5)-(10) at the Ω boundary. Let λ_{α_1} and λ_{α_2} be the nearest to α^2 eigenvalues λ_k so that

$$\lambda_{\alpha_1} \,<\, \alpha^2 \,<\, \lambda_{\alpha_2}. \tag{29}$$

Since $\alpha^2 > \delta$ and the operator $\mathcal{A}\,u$ is non-sign-definite one, its eigenvalues $\mu_k = \lambda_k - \alpha^2$ are located within two intervals such as

$$\hat{\gamma_1} \,\le\, \hat{\gamma_2} \,<\, 0 \,<\, \hat{\gamma_3} \,\le\, \hat{\gamma_4}. \tag{30}$$

¿From (15), (18), (19) and (29) we have

$$\hat{\gamma_1} = \delta - \alpha^2,\ \hat{\gamma_2} = \lambda_{\alpha_1} - \alpha^2,\ \hat{\gamma_3} = \lambda_{\alpha_2} - \alpha^2,\ \hat{\gamma_4} = \Delta - \alpha^2. \tag{31}$$

It may be shown (Samarsky and Nikolaev, 1978) that the best evaluation for β in (28) is

$$\beta \equiv \beta_0 = (\hat{\gamma_2} + \hat{\gamma_3})/2 \tag{32}$$

and the limits of the spectrum of eigenvalues of the operator $\hat{\mathcal{A}}$ are:

$$\gamma_1 = (\alpha^2 - \lambda_{\alpha_1})\,(\lambda_{\alpha_2} - \alpha^2) \tag{33}$$

$$\gamma_2 = \begin{cases} (\triangle - \alpha^2)\,(\triangle + \alpha^2 - \lambda_{\alpha_1} - \lambda_{\alpha_2}) & \text{if } \lambda_{\alpha_1} + \lambda_{\alpha_2} \leq (\triangle + \delta) \\ (\alpha^2 - \delta)\,(\lambda_{\alpha_1} + \lambda_{\alpha_2} - \alpha^2 - \delta) & \text{if } \lambda_{\alpha_1} + \lambda_{\alpha_2} \geq (\triangle + \delta) \end{cases} \tag{34}$$

The sequence of iteration parameters $\{\tau_m\}$ is given by

$$\begin{aligned} \tau_{2m-1} &= -\beta_0\,\omega_m - \sqrt{\beta_0^2\,\omega_m^2 + \omega_m}, \\ \tau_{2m} &= -\beta_0\,\omega_m + \sqrt{\beta_0^2\,\omega_m^2 + \omega_m}, \\ m &= 1, 2, \ldots, n, \end{aligned} \tag{35}$$

where

$$\omega_m = \frac{\omega_0}{1 + \rho_0 \nu_m},\ \nu_m \in \mathcal{M}_n = \{-\cos\frac{(2i-1)\pi}{2n},\ 1 \leq i \leq n\},\ 1 \leq m \leq n$$

$$\omega_0 = \frac{2}{\gamma_1 + \gamma_2},\ \rho_0 = \frac{1-\xi}{1+\xi},\ \xi = \frac{\gamma_1}{\gamma_2}.$$

n is estimated by (24) with ρ_1 defined by (25), where γ_1 and γ_2 are given by (33)-(34). Note that the length of the sequence of iteration parameters (35) at least twice as many as n.

Further, as well as in the case of positive-definite operator $\mathcal{A}\,u$, according to the iteration scheme (20), where the operator $\mathcal{A}$ on the grid ω is determined by (14), the approximate solution B_z to the Helmholtz equation (13) may be calculated.

2.2 Calculation of B_x and B_y

¿From (1)-(2) we have

$$\frac{\partial B_y}{\partial x} - \frac{\partial B_x}{\partial y} = \alpha\,B_z \tag{36}$$

$$\frac{\partial B_x}{\partial x} + \frac{\partial B_y}{\partial y} + \frac{\partial B_z}{\partial z} = 0 \tag{37}$$

If $\partial^2 B_y/\partial x \partial y$ is continuous function, then $\partial^2 B_y/\partial x \partial y = \partial^2 B_y/\partial y \partial x$, and from (36)- (37) we get

$$\frac{\partial^2 B_x}{\partial x^2} + \frac{\partial^2 B_x}{\partial y^2} = -\frac{\partial^2 B_z}{\partial x \partial z} - \alpha \frac{\partial B_z}{\partial y}, \tag{38}$$

or

$$\nabla^2 B_x = -\phi(x, y), \tag{39}$$

where

$$\phi(x, y) \equiv \frac{\partial^2 B_z}{\partial x \partial z} + \alpha \frac{\partial B_z}{\partial y}$$

is known function of (x, y) at every level of the grid ω along the z-axis, since B_z are now known throughout the volume of integration.

Thus, on selected plane $z = z^*$ for B_x the $2D$ Dirichlet boundary value problem for the Poisson equation (39) is stated. The boundary conditions are specified by (11). To solve this DBVP the routine proposed above can be used in $2D$ modification. The difference analogue of the differentiation operator

$$A\,u = \frac{\partial^2 u}{\partial x^2} + \frac{\partial^2 u}{\partial y^2} + \phi(x, y)$$

we specified as

$$\begin{aligned} \mathcal{A}\,u &= (u_{i+1,j} - 2u_{i,j} + u_{i-1,j})/h_1^2 + \\ & \quad (u_{i,j+1} - 2u_{i,j} + u_{i,j-1})/h_2^2 + \phi_{i,j} \\ & \quad i = 2, 3 \ldots, n_1 - 1,\ j = 2, 3 \ldots, n_2 - 1. \end{aligned} \tag{40}$$

Lower and upper bounds of the spectrum of the operator (40) are:

$$\gamma_1 \equiv \delta = \sum_{\gamma=1}^{2} \frac{4}{h_\gamma^2} \sin^2(\pi/2n_\gamma), \tag{41}$$

$$\gamma_2 \equiv \Delta = \sum_{\gamma=1}^{2} \frac{4}{h_\gamma^2} \cos^2(\pi/2n_\gamma), \tag{42}$$

Operator (40) is positive-definite, so we can use the iteration routine presented in Subsection 2.1.1. Parameters for iteration scheme can be determined by the same expressions (21), (22), (24), (25), (27) with γ_1 and γ_2 obtained by (41),(42).

Similarly, the Dirichlet boundary value problem for B_y component at the plane $z = z^*$ with boundary conditions (12) can be stated. The function $\phi(x, y)$ will be:

$$\phi(x, y) = \frac{\partial^2 B_z}{\partial z \partial y} - \alpha \frac{\partial B_z}{\partial y} \tag{43}$$

Now we have $B_x\ (x, y, z^*)$ and $B_y\ (x, y, z^*)$ at the chosen plane $z = z^*$. To find B_x and B_y throughout the volume Ω we used a representation of $\mathbf{B}$ (Seehafer, 1978):

$$\mathbf{B} = \alpha \mathbf{e}_z \times \nabla P + \nabla \times (\mathbf{e}_z \times \nabla P), \tag{44}$$

where P is a generating function which satisfies the Helmholtz equation and $\mathbf{e}_z$ is the unit vector in the z direction. From (44) we get

$$B_x = -\alpha \frac{\partial P}{\partial y} - \frac{\partial^2 P}{\partial x \partial z} \tag{45}$$

$$B_y = \alpha \frac{\partial P}{\partial x} - \frac{\partial^2 P}{\partial y \partial z} \tag{46}$$

$$B_z = -\alpha^2 P - \frac{\partial^2 P}{\partial z^2}. \tag{47}$$

The general solution to Eq. (47) can be written in the form:

$$P(x, y, z) = P_0(x, y, z) + C_1(x, y) \cos \alpha z + C_2(x, y) \sin \alpha z, \tag{48}$$

where $C_1(x,y)$ and $C_2(x,y)$ are unknown functions, and $P_0(x,y,z)$ denotes a particular solution to Eq. (47). Let

$$P_0(x,y,z) = \frac{\cos\alpha z}{\alpha}\int_{z_0}^{z} B_z(x,y,\zeta)\sin\alpha\zeta\,\mathrm{d}\zeta - \frac{\sin\alpha z}{\alpha}\int_{z_0}^{z} B_z(x,y,\zeta)\cos\alpha\zeta\,\mathrm{d}\zeta. \tag{49}$$

Putting the expression (48) into (45) and (46) we get

$$-\frac{\cos\alpha z}{\alpha}B_x + \frac{\sin\alpha z}{\alpha}B_y = d_1(x,y) + q_1(x,y,z) \tag{50}$$

$$\frac{\sin\alpha z}{\alpha}B_x + \frac{\cos\alpha z}{\alpha}B_y = d_2(x,y) + q_2(x,y,z), \tag{51}$$

where

$$q_1(x,y,z) = -\frac{\sin\alpha z}{\alpha}\frac{\partial^2 P_0}{\partial y\partial z} + \sin\alpha z\frac{\partial P_0}{\partial x} + \frac{\cos\alpha z}{\alpha}\frac{\partial^2 P_0}{\partial x\partial z} + \cos\alpha z\frac{\partial P_0}{\partial y} \tag{52}$$

$$q_2(x,y,z) = -\frac{\cos\alpha z}{\alpha}\frac{\partial^2 P_0}{\partial y\partial z} + \cos\alpha z\frac{\partial P_0}{\partial x} - \frac{\sin\alpha z}{\alpha}\frac{\partial^2 P_0}{\partial x\partial z} - \sin\alpha z\frac{\partial P_0}{\partial y} \tag{53}$$

can be determined from B_z throughout the Ω; and

$$d_1(x,y) \equiv \frac{\partial C_1}{\partial y} + \frac{\partial C_2}{\partial x} \tag{54}$$

$$d_2(x,y) \equiv -\frac{\partial C_2}{\partial y} + \frac{\partial C_1}{\partial x} \tag{55}$$

are unknown functions which do not depend from z. They can be determined by (50)-(51) written for the chosen plane $z = z^*$, since $B_x(x,y,z^*)$ and $B_y(x,y,z^*)$ are known.

Now we can determine $B_x(x,y,z)$ and $B_y(x,y,z)$ throughout the volume Ω by the same (50)-(51) written as

$$B_x(x,y,z) = \alpha\sin\alpha z\left[d_2(x,y) + q_2(x,y,z) - \frac{\cos\alpha z}{\sin\alpha z}(d_1(x,y) + q_1(x,y,z))\right] \tag{56}$$

$$B_y(x,y,z) = \frac{\alpha}{\sin\alpha z}\left[d_1(x,y) + q_1(x,y,z) + \frac{\cos\alpha z}{\alpha}B_x(x,y,z)\right]. \tag{57}$$

3 Accuracy of the proposed method

To estimate the accuracy of the algorithm it is convenient to use a routine proposed by Cuperman, Ofman and Semel (1989, refered to as Paper I) for a comparison between numerical and analytical solutions to LFFF equations.

The exact solution to the LFFF equations in a half-space have been obtained by Chiu and Hilton (1977). We shall use it for a simplest case when B_z are non-zero only in two pixels of the grid. Following Paper I, let us consider a situation when at the bottom (the plane $z = 0$) of the rectangular box Ω B_z are specified, and $B_z \neq 0$ only at two points: $(-d,\,0,\,0)$, and $(d,\,0,\,0)$. (The Cartesian coordinate origin is located at the center of the

Ω bottom, see Figure 1 in Paper I.) Let $B_z(-d,\,0,\,0) = -B_z(d,\,0,\,0)$. Then by making use of (13)-(16) from Chiu and Hilton (1977) for a half-space above some plane $z = z_0 > 0$ one can calculate the linear force-free field generated by every "pole" at a point $(x,\,y,\,z)$ (see also (22)-(24) in Paper I):

$$\begin{aligned}
B_{x,j} &= \frac{1}{r_j^2}[x_j\frac{r_j^2}{R_j^2}\cos(\alpha R_j) - \alpha\frac{x_j z^2}{R_j^2}\sin(\alpha R_j) + \\
&\quad \alpha x_j \sin(\alpha z) + \alpha\frac{yz}{R_j}\cos(\alpha R_j) - \alpha y\cos(\alpha z)] \qquad (58)\\
B_{y,j} &= \frac{1}{r_j^2}[y_j\frac{r_j^2}{R_j^2}\cos(\alpha R_j) - \alpha\frac{y\,z^2}{R_j^2}\sin(\alpha R_j) + \\
&\quad \alpha y \sin(\alpha z) - \alpha\frac{x_j z}{R_j}\cos(\alpha R_j) - \alpha x_j\cos(\alpha z)] \qquad (59)\\
B_{z,j} &= \frac{z}{R_j^3}[\cos(\alpha R_j) + \alpha R_j\sin(\alpha R_j)] \qquad (60)
\end{aligned}$$

where

$$j = 1,2;\; R_j^2 = r_j^2 + z^2,\; r_j^2 = x_j^2 + y^2,\; x_1 = x - d,\; x_2 = x + d.$$

The resultant B_x, B_y, B_z – components at a point $(x,\,y,\,z)$ are

$$\begin{aligned}
B_x &= B_{x,1} - B_{x,2}, \qquad (61)\\
B_y &= B_{y,1} - B_{y,2}, \qquad (62)\\
B_z &= B_{z,1} - B_{z,2}.. \qquad (63)
\end{aligned}$$

Following Paper I, the distances $x,\,y,\,z,\,r_j,\,R_j$ in Eqs. (58)-(60) are normalized to L_0 — the depth of the "poles" descending beneath the "photospheric" surface $z = z_0$; thus, $z_0 = 1$. We have taken $\alpha = 1$ and $d = 1/9$, the rectangular box Ω: $\{-3 \le x \le 3;\ -3 \le y \le 3;\ 1 \le z \le 4;\}$. A horizontal mesh of $n_1 \times n_2 = 51 \times 51$ grid points was used; thus, $h_1 = h_2 = 0.12$. The vertical grid spacing used was taken as $h_3 = 0.1$; thus, $n_3 = 31$.

Analytical solution $\mathbf{B}$ to the LFFF equations inside the Ω was calculated by (58)-(63).

Numerical solution $\mathbf{B}'$ to the LFFF equations (1)- (3) inside the Ω was obtained by Chebyshev's iteration method. The boundary conditions (5)-(12) were calculated by the analytical formulae (58)-(63). z^* was taken as 4.0. On the given mesh the minimum eigenvalue of the $3D$ Laplacian $\delta = 1.64$, thus, $\alpha^2 < \delta$, and the $3D$ difference operator $\mathcal{A}u$ defined in (14) is positive-definite one. With $\varepsilon = 10^{-4}$ a total number of iteration n according to (24) has not to be less than $n_0 = 190$.

The deviation of the analytical solution $\mathbf{B}$ from the numerical $\mathbf{B}'$ was estimated by the formula (28) of Paper I which gives the average of the relative error over the entire horizontal plane of integration domain $\langle \triangle B_\gamma \rangle$ $(\gamma = x,\,y,\,z)$ as a function of height z:

$$\langle \triangle B_\gamma \rangle = \frac{1}{\langle B_\gamma \rangle}\left[\sum_{i=1}^{n_1}\sum_{j=1}^{n_2}(B_{\gamma;i,j} - B'_{\gamma;i,j})^2/(n_1 \times n_2)\right]^{1/2}. \qquad (64)$$

The functions calculated by this way are presented in Figure 1. One can see that the maximum values of $\langle \triangle B_\gamma \rangle$ are about 0.9% at $z = 1.1$ for $\langle \triangle B_x \rangle$, about 0.6% at $z = 1.1$ for $\langle \triangle B_y \rangle$, and about 0.4% at $z = 3.2$ for $\langle \triangle B_z \rangle$.

Thus, the proposed numerical method ensures a good enough accuracy of the linear force-free field reconstruction.

4 Potential Non-Photospheric Boundary Conditions

Expressions (58)-(63) give an analytical representation of a field that is a linear force-free in a half-space $z > z_0$. The solution $\mathbf{B}^{'}$ obtained in the previous section is a fragment of such a field inside the volume Ω (with the accuracy better than 1%), since the boundary conditions (5)-(12) were defined by (58)-(63).

Let us specify another boundary conditions (5)-(12), say, potential field values. Then

$$\psi_i = B_z(pot) \text{ for } i = 2, ..., 6 \text{ in } (6) - (10);$$

$$g_1(x, y)|_G = B_x(pot) \text{ in } (11),$$
$$g_2(x, y)|_G = B_y(pot) \text{ in } (12).$$

$\psi_1(x, y)$ in (5) let be the same as in $\mathbf{B}^{'}$ calculations. z^* let be also equal to 4.0. Taking such boundary conditions we calculated $\mathbf{B}^{''}$ and compared it with $\mathbf{B}^{'}$. Potential field was calculated by B_z (at $z_0 = 1$) as a boundary conditions using our modification of the Schmidt integration method (Abramenko, 1986).

Starting from the same B_z magnetogram at $z = z_0 = 1.0$ the fields $\mathbf{B}^{'}$ and $\mathbf{B}^{''}$ exhibit quite different behaviors with height. B_z – components and orientation of transverse field vector $\mathbf{B}_\perp$ of $\mathbf{B}^{'}$ and $\mathbf{B}^{''}$ in the (x, y) planes at three heights are shown in Figure 2. For the $B_z^{'}$ (Figure 2a), areas of main fluxes decrease and areas of opposite polarity increase with height. Whereas for the $B_z^{''}$, the sign of $B_z^{''}$ preserves up to $z = 3.9$. Vortices of $\mathbf{B}_\perp^{'}$ and $\mathbf{B}_\perp^{''}$ (Figure 2b) also are quite different. Such an obvious difference between $\mathbf{B}^{'}$ and $\mathbf{B}^{''}$ in vertical and transverse field components implies that the magnetic flux tube structures of $\mathbf{B}^{'}$ will deviate from those of $\mathbf{B}^{''}$. This is confirmed by Figure 3 where the lines of force for $\mathbf{B}^{'}$ and $\mathbf{B}^{''}$ are shown. Field lines of $\mathbf{B}^{'}$ and $\mathbf{B}^{''}$ were integrated from the start points with the same (x, y) coordinates, but the main flux tube of $\mathbf{B}^{''}$ is more extensive, more high and has another twist.

Thus, magnetic field configurations $\mathbf{B}^{'}$ and $\mathbf{B}^{''}$ calculated by the same numerical routine at the same volume by the same photospheric B_z, but having different boundary conditions at non-photospheric sides of the volume, significantly differ.

5 Conclusions

We have proposed here the technique which renders to calculate a linear force-free magnetic field inside a bounded domain (as a rectangular box Ω) provided B_z component is prescribed at all sides of the Ω and B_x, B_y are specified on the intersection of the lateral part of the Ω boundary with one selected plane $z = const$. Such a routine may be useful when, modelling a LFFF above a limited region of the solar photosphere, there is some *a priori* information about the field at non-photospheric boundaries of the studied volume.

The routine also may be used under the assumption that B_z vanish at vertical and top sides of the volume Ω.

The method given here renders it possible to broad the integration domain without decreasing of the region of accessible α except one requirement: α has not to coincide precisely with any eigenvalue of the $3D$ Laplacian. The algorithm does not imply any periodicity of observational data and of the solution beyond the magnetogram as Fourier transform method does.

The simplest numerical example (Section 4) shown that the taking into account *a priori* informations about the field values in the corona may change considerably the results of LFFF modeling in an active region.

The authors are very grateful to the referee, whose comments and suggestions have led to a substantial improvement of this paper. This research was supported by the grant of American Astronomical Society.

A Arrangement of the Set $\mathcal{M}_n$

Let n be the number of iterations estimated by (24).Let us denote as Θ^m a set of m integer numbers:

$$\Theta^m = \left\{\Theta_1^{(m)}, \Theta_2^{(m)}, \ldots, \Theta_m^{(m)}\right\}$$

Starting from $\Theta^1 = \{1\}$, let us determine a procedure forming a set Θ^n by the following way. Individual steps of this procedure are transitions of two kinds: a transition from Θ^m to Θ^{2m} and a transition from Θ^{2m} to Θ^{2m+1}.

The transition from Θ^{2m} to Θ^{2m+1} is to add the odd number $2m+1$ behind a last element of Θ^{2m}.

The transition from Θ^m to Θ^{2m} is more complex one. If it is followed by $\Theta^{2m} \to \Theta^{4m}$, or if it is the last step in Θ^n formation, then

$$\Theta_{2i-1}^{(2m)} = \Theta_i^{(m)}, \quad \Theta_{2i-1}^{(2m)} + \Theta_{2i}^{(2m)} = 4m, \quad i = 1, 2, \ldots, m;$$

if it is followed by $\Theta^{2m} \to \Theta^{2m+1}$, than

$$\Theta_{2i-1}^{(2m)} = \Theta_i^{(m)}, \quad \Theta_{2i-1}^{(2m)} + \Theta_{2i}^{(2m)} = 4m + 2, \quad i = 1, 2, \ldots, m.$$

To make things clear let us consider a simple example for $n = 15$. A sequence of transitions from Θ^1 to Θ^{15} will be so far: $\Theta^1 \to \Theta^2 \to \Theta^3 \to \Theta^6 \to \Theta^7 \to \Theta^{14} \to \Theta^{15}$. This sequence is obvious if one looks at it in the inverse order. According to the above rule, the sets Θ^m $(m = 1, 2, 3, 6, 7, 14, 15)$ are

$\Theta^1 = \{1\}$;
$\Theta^2 = \{1, 5\}$;
$\Theta^3 = \{1, 5, 3\}$;
$\Theta^6 = \{1, 13, 5, 9, 3, 11\}$;
$\Theta^7 = \{1, 13, 5, 9, 3, 11, 7\}$;
$\Theta^{14} = \{1, 29, 13, 17, 5, 25, 9, 21, 3, 27, 11, 19, 7, 23\}$;
$\Theta^{15} = \{1, 29, 13, 17, 5, 25, 9, 21, 3, 27, 11, 19, 7, 23, 15\}$;

Using the formed set Θ^n, let us arrange the set

$$\mathcal{M}_n = \{-\cos \frac{2i-1}{2n}\,\pi,\ i = 1, 2, \ldots, n\}$$

by the following way:

$$\mathcal{M}_n^* = \left\{-\cos\left(\beta_i\right),\ \beta_i = \frac{\pi}{2n}\,\Theta_i^{(n)},\ i = 1, \ldots, n\right\}.$$

Now, when forming the sequence of iteration parameters by (21), one can take consecutively elements of the ordered set $\mathcal{M}_n^*$ as ν_m, then the iteration process is stable one, and minimal calculation errors are ensured.

References

Abramenko, V.I.: 1986, *Soln. Dann.* **8**, 83.

Alissandrakis, C.E.: 1993, in G. Belvedere, M. Rodono, G.M. Simnett (eds.) *"Advances in*

Solar Physics" Lecture Notes in Physics **432**, 109.

Aly, J.J., Seehafer, N.: 1993, *Solar Phys.* **144**, 243.

Chiu, Y.T., Hilton, H.H.: 1977, *Astrophys. J.* **212**, 873.

Cuperman, S., Ofman, L., Semel, M.: 1989, *Astron. and Astrophys.* **216**, 265.

Sakurai, T.: 1989, *Space Sci. Rev.* **51**, 11.

Samarsky, A.A., Nikolaev, E.S.: 1978, *Methods of the solution of grid equations*, Moscow: "Nauka", 588p.

Seehafer, N.: 1978, *Solar Phys.* **58**, 215.

Seehafer, N.: 1982, *Solar Phys.* **81**, 69.

Seehafer, N., Staude, J.: 1983, *Physica Solari-Terrestris.* **N22**, 5.

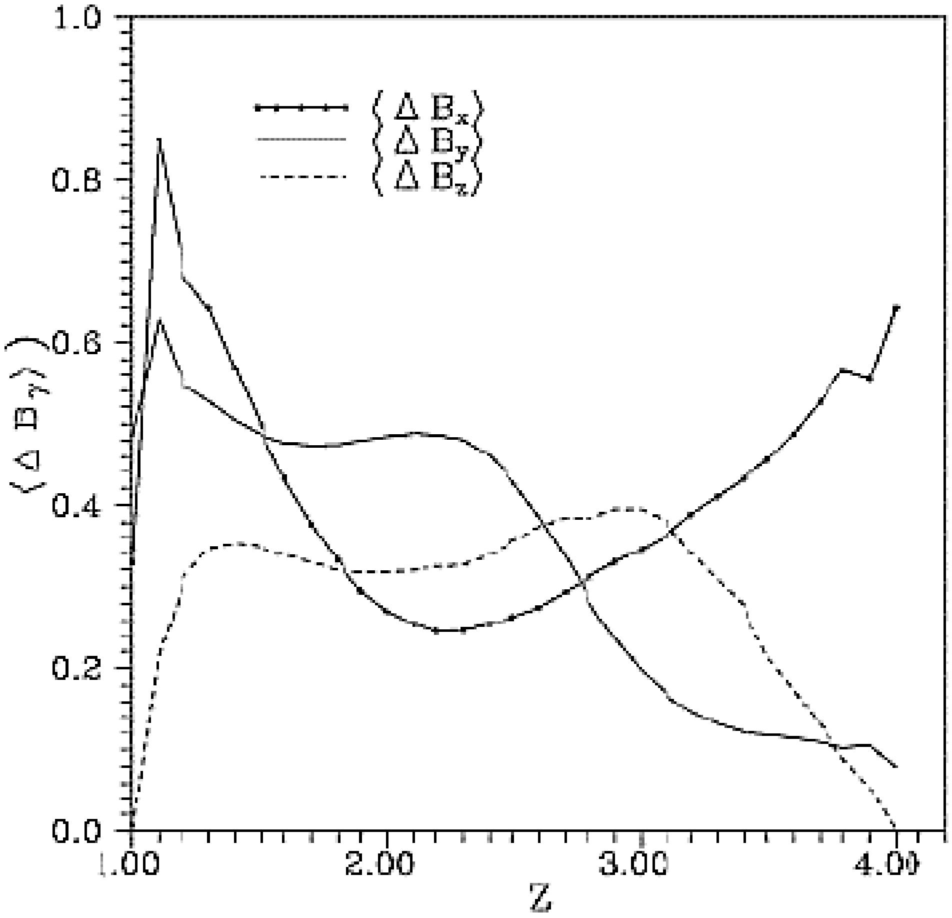

Figure 1. Average over the entire horizontal plane of the integration domain of the relative error $\langle \triangle B_\gamma \rangle$ ($\gamma = x,\, y,\, z$) of the numerical solution $\mathbf{B}'$ relative to the analytic solution $\mathbf{B}$ as a function of z

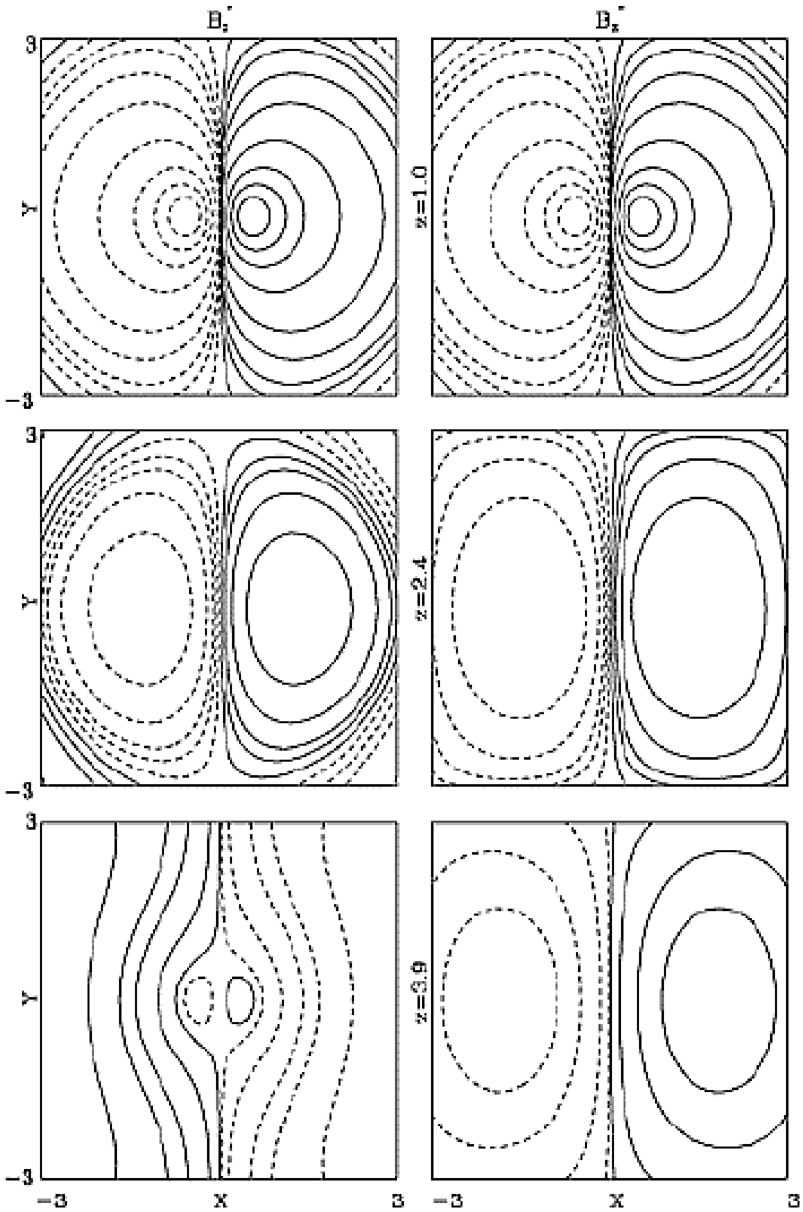

Figure 2a. Contours of B_z magnetic field component (a) and azimuth of total transverse field vector (b) in the (x, y) planes situated at the heights indicated on the frames for $\mathbf{B}'$ — linear force-free field with analytic force-free boundary conditions and for $\mathbf{B}''$ — linear force-free field with potential non-photospheric boundary conditions. Solid (dashed) lines indicate positive (negative) fields. Contour levels are drown at ± 10, ± 30, ± 50, ± 100, ± 200, ± 500, ± 1000, ± 1500, ± 2000 units; the contour ± 1 is added at $z = 3.9$

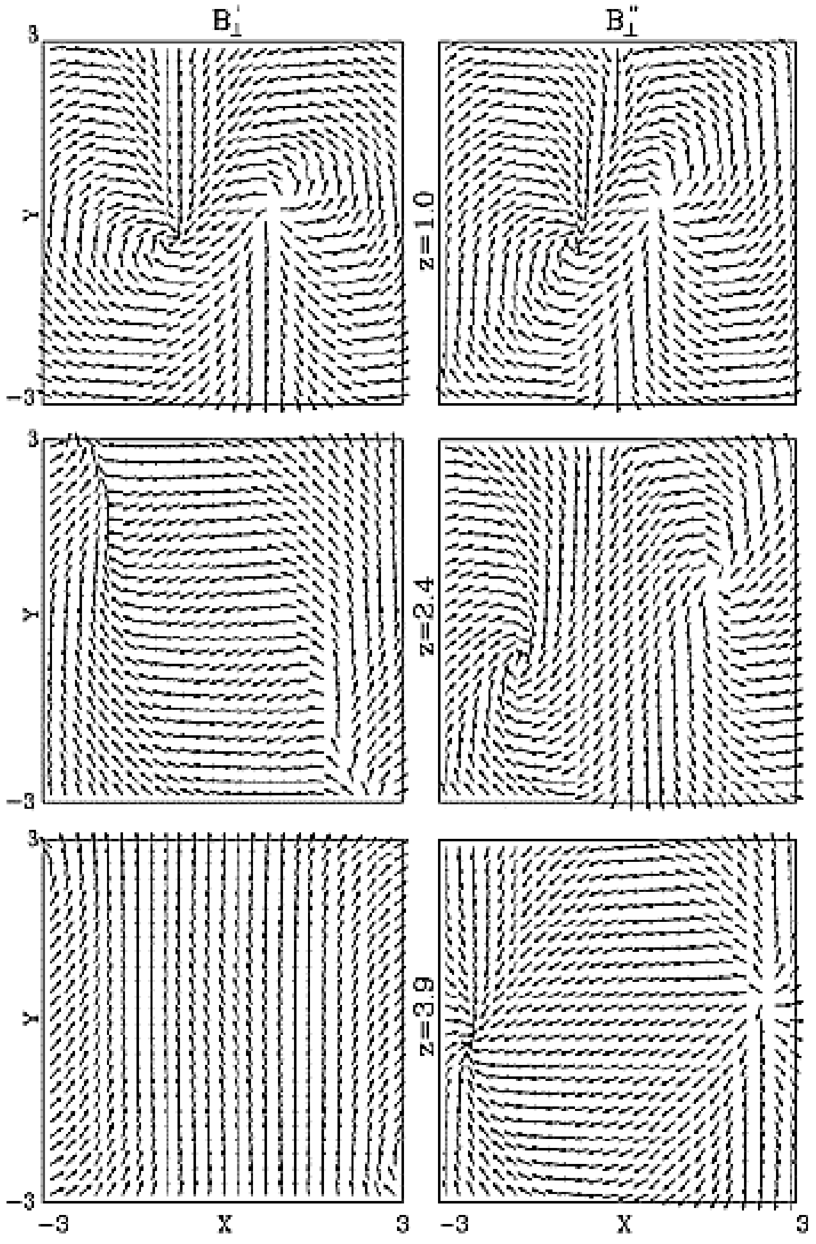

Figure 2b. Contours of B_z magnetic field component (a) and azimuth of total transverse field vector (b) in the $(x,\,y)$ planes situated at the heights indicated on the frames for $\mathbf{B}'$ — linear force-free field with analytic force-free boundary conditions and for $\mathbf{B}''$ — linear force-free field with potential non-photospheric boundary conditions. Solid (dashed) lines indicate positive (negative) fields. Contour levels are drown at ± 10, ± 30, ± 50, ± 100, ± 200, ± 500, ± 1000, ± 1500, ± 2000 units; the contour ± 1 is added at $z = 3.9$

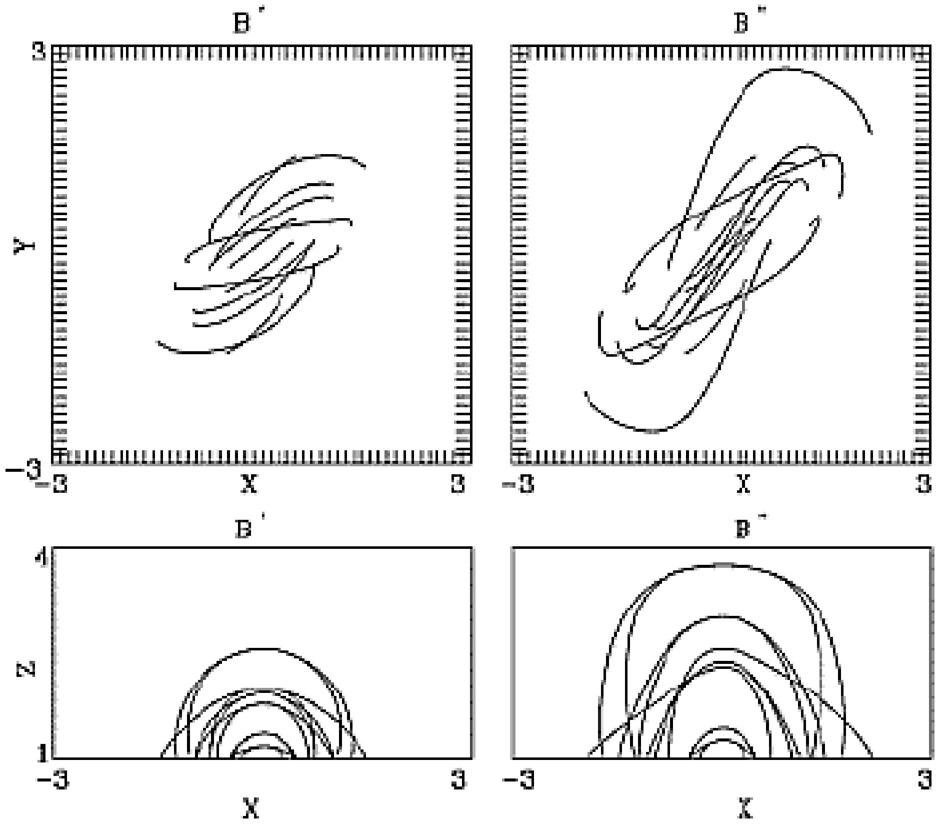

Figure 3. Topview (*top panel*) and sideview (*bottom panel*) of the lines of force above the region of Figure 2 for the fields $\mathbf{B}^{'}$ and $\mathbf{B}^{''}$ mentioned in the Figure 2 caption